

ACCELERATION EFFECT ON FLUID FORCES ACTING ON THE HAND IN SWIMMING

Shigetada Kudo, Ross Vennell*, and Barry Wilson**

School of Sports, Health & Leisure, Republic Polytechnic, Singapore, Singapore

School of Physical Education, University of Otago, Dunedin, New Zealand

*Department of Marine Science, University of Otago, Dunedin, New Zealand

** National Institute of Sport, Kuala Lumpur, Malaysia

This study aimed to quantify and investigate the effect of acceleration on fluid forces acting on a hand model. An accelerating hand in swimming generates large fluid forces in a stroke, although the effect of acceleration on fluid forces on the hand has not been well quantified. An experiment rotating a hand model in a flowing flume was conducted to measure fluid forces on the hand model and pressure on the hand surface. The effect of acceleration on fluid forces acting on the hand was quantified based on a theoretical understanding in fluid mechanics. Accelerated motion induced additional fluid forces on the hand, consistent with the theoretical understanding while decelerated motion induced additional fluid forces, not consistent with the theoretical understanding. Dynamic pressures measured were attributed to the formation of large vortices, inducing the additional fluid forces.

KEYWORDS: Inertia coefficient, deceleration, non-accelerating and accelerating hand

INTRODUCTION:

The hands are an important contributor to propulsion in the front crawl stroke. Forces exerted by the hands have been quantified based on the coefficient of fluid forces known as the quasi-static approach (Schleihauf, 1979), and the results have been applied to the technical recommendations for the stroke. However, the accelerating hand in swimming needs to be considered for the quantification of fluid forces acting on the hand (Pai & Hay, 1988). The effect of acceleration on fluid forces acting on the hand in swimming has not yet been well quantified. The aim of the present study was to quantify and investigate the effect of acceleration on fluid forces (H) acting on a hand model. The findings were expected to result in a better understating of the generation of fluid forces on the hand in swimming.

METHOD: Experiments were conducted in a flowing flume at a constant speed, so as to measure the pressure on the surface of a hand model and the resultant fluid force acting on the hand model in accelerated and non-accelerated motion (Fig. 1). Five pressure sensors (KYOWA, Tokyo, Japan) were used to measure pressure on the surface of the hand model as shown in Fig. 1. The locations were the side of head of the fifth metacarpal for one sensor (p_3) and the head of the third and fourth metacarpal (p_1 and p_2 on the ventral side and p_5 and p_4 on the dorsal side) for four sensors. The pressure values were used to deduce the flow conditions around the hand model. The hand model was attached to a load cell (AMTI, Massachusetts, USA) by a stainless bar that was covered by a hollow cylindrical model "forearm". The model forearm was fixed so as to not affect the values measured in the load cell. A thin elastic material made watertight covered the gap between the hand model and the model forearm. Thus, the present study derived only fluid forces acting on the hand model using the equation of motion in the t -direction perpendicular to the model's longitudinal axis (H_t). The angular position of the model (ϕ) was measured by a potentiometer. The orientation of the hand model was with the hand surface perpendicular to the model rotation plane. The flow speed relative to the hand model, U , was calculated from the velocity in the flume and the velocity of the hand model. The angle of incidence, β , was defined as the angle between the model's longitudinal axis and the flow direction relative to the hand. β was defined as 0° when the direction of flows relative to the hand model was parallel to the longitudinal axis and toward the rotation axis and was 90° when the relative flow direction was perpendicular to the longitudinal axis and toward the palm side. The flow

speed in the flume and the amount of driving masses were changed to produce various values of U and acceleration in the t -direction, a_t , for the accelerating hand testing.

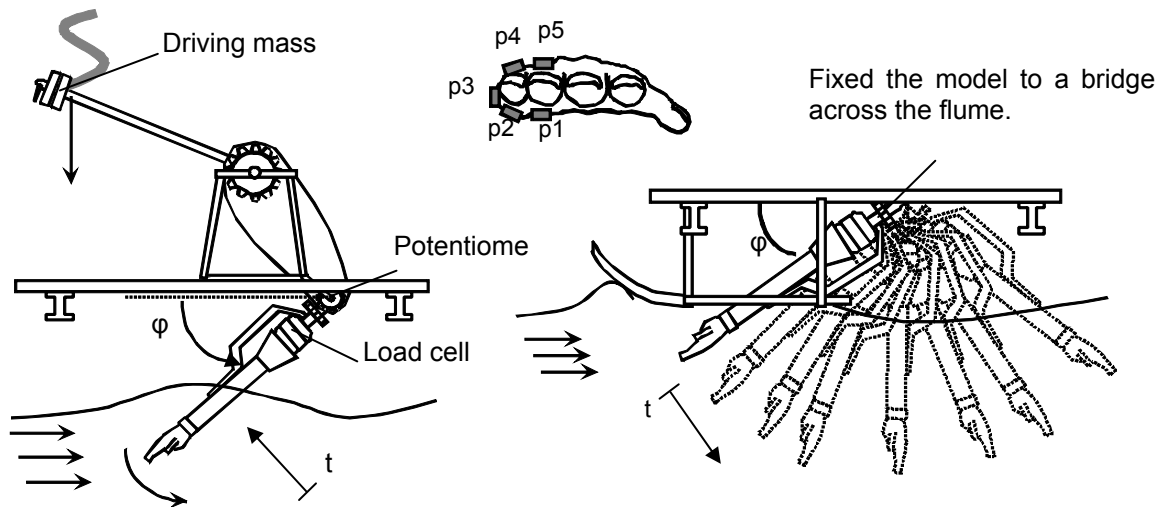


Figure 1: The left figure shows the accelerating hand in testing, and the right shows the non-accelerating hand in testing. The top-middle shows the location of pressure sensors.

Fluid forces acting on the hand model in accelerated motion were expressed by the following equation (Daniel, 1984; Morison, O'Brien, Johnson, & Schaaf, 1950):

$$H_t = \rho V C_i^t a_t + 0.5 \rho A C_d^t U^2 \quad (1)$$

where ρ is the density of fluid, V is the hand volume, C_i^t is the inertia coefficient, A is the hand area, and C_d^t is the coefficient of fluid force in the t -direction.

The values of C_i^t and C_d^t were determined from all trials of differing U and a_t for each β from 10° to 130° in 10° increments. H_t was predicted by data in the non-accelerating hand (H_t^0), and the difference between H_t and H_t^0 was calculated ($H_t - H_t^0$).

Knowing hydrostatic pressures from the depth of the hand model, hydrodynamic pressures were derived by subtracting the hydrostatic pressures from the pressures measured by the pressure sensors. Using the dynamic pressure in the non-accelerating hand, the dynamic pressure for the accelerating hand model was predicted (p^0).

RESULTS:

The value of C_i^t increased until $\beta = 60^\circ$ (4.0) in the early phase of model rotation and then decreased until $\beta = 100^\circ$ (-3.3) in the late phase while the average of a_t changed from -4 m/s^2 to 13 m/s^2 (Figs. 2 and 3). The value of $H_t - H_t^0$ increased as a_t increased when C_i^t was maximum ($\beta = 60^\circ$), and the value of $H_t - H_t^0$ increased as a_t decreased when C_i^t was minimum ($\beta = 100^\circ$) as shown in Fig. 4 and Fig. 5, respectively. The maximum $H_t - H_t^0$ at $\beta = 60^\circ$ was 26 N ($H_t = 33 \text{ N}$ and $H_t^0 = 7 \text{ N}$), and the maximum $H_t - H_t^0$ at $\beta = 100^\circ$ was 49 N ($H_t = 107 \text{ N}$ and $H_t^0 = 58 \text{ N}$).

DISCUSSION:

$H_t - H_t^0$ increased as a_t increased at $\beta = 60^\circ$ (Fig. 4). H_t was approximately 4 times greater than H_t^0 . The value of a_t was large and positive when β became maximum at 60° . The results are consistent with the theoretical understanding that fluid forces acting on an object increase due to the acceleration reaction for the positive accelerated motion (Daniel, 1984). As shown in Fig. 5, $H_t - H_t^0$ increased as a_t decreased. H_t was approximately 2 times greater than H_t^0 while the magnitude was larger than that for $\beta = 60^\circ$. The value of a_t was small or negative when β became minimum at 100° . The results are not consistent with the theoretical understanding because H_t increased while a_t decreased.

In the present study, H_t depended on the pressure difference between the dorsal and ventral sides of the hand model since U was relatively fast (high Reynolds number). The pressure

distribution around the hand model should be influenced by flow conditions around the model. Thus, the pressure values measured were used to deduce flow conditions around the hand model (Figs. 6 and 7). At $\beta = 60^\circ$ as shown in Fig. 6, the largely different value between p_4 and p_4^0 and the decrease in pressure from p_3 to p_5 indicates that large attached vortices involving high intensity and velocity flow might be generated inducing additional H_t as seen in Figs. 4. The impulsive-started motion induces large attached vortices behind a blunt object and additional fluid forces on the object (Sarpkaya & Isaacson, 1981). At $\beta = 100^\circ$ as shown in Fig. 7, the values of p_4 and p_5 were much lower than those of p_4^0 and p_5^0 . The larger pressure difference in the accelerating hand model than for the non-accelerating hand model was due to the large magnitude of negative pressure on the dorsal side of the hand model. The negative pressure may be due to the generation of large vortices since, although the study of Maresca, Favier, & Rebont (1979) used an aerofoil set at 20° of angle of attack, the previous study showed that vortices behind the aerofoil disintegrated in decelerated motion, and fluid forces on the aerofoil and the magnitude of negative pressure on the dorsal side of the aerofoil became much larger than for the steady case.

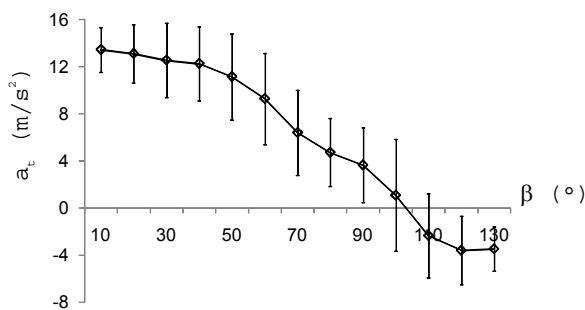


Figure 2: The value of a_t for various β

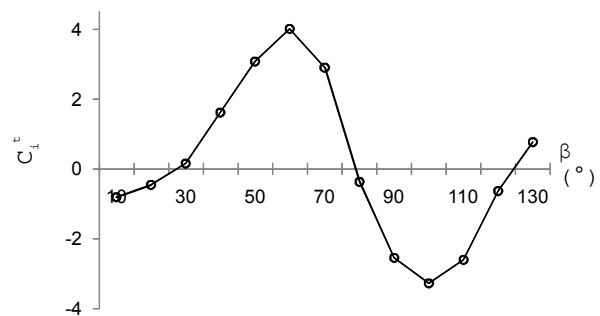


Figure 3: The value of C_t^t for various β

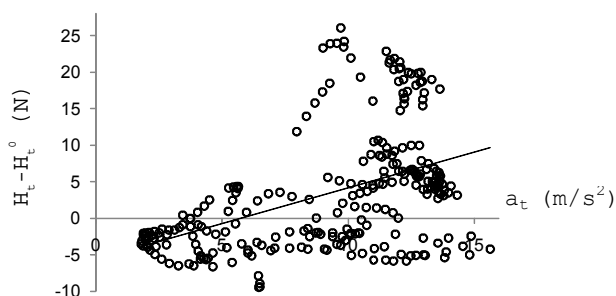


Figure 4: The value of $H_t - H_t^0$ as a function of a_t at $\beta = 60^\circ$

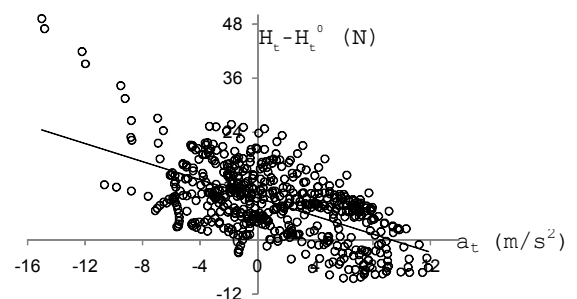


Figure 5: The value of $H_t - H_t^0$ as a function of a_t at $\beta = 100^\circ$

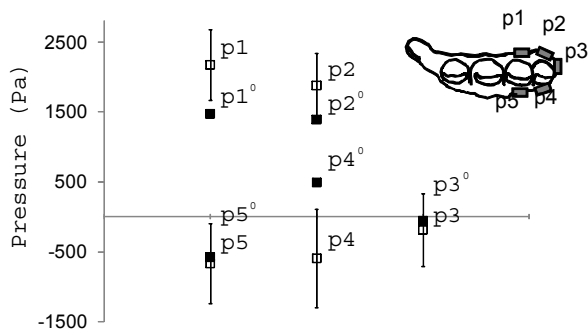


Figure 6: Pressure at the various sensors at $\beta = 60^\circ$

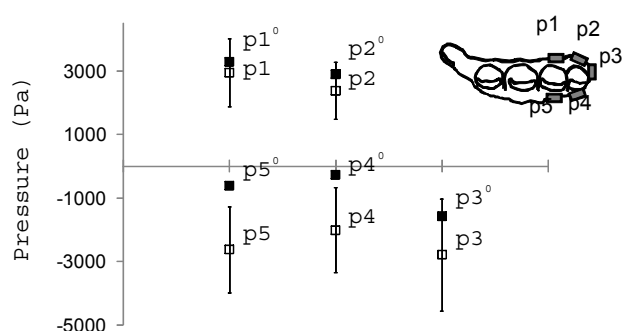


Figure 7: Pressure at the various sensors at $\beta = 100^\circ$

CONCLUSION:

Accelerated motion induces additional fluid forces on the hand in swimming up to 4 times larger than non-accelerated motion. The theory for decelerated hand motion needs to be developed for understanding the mechanism of additional fluid forces on the hand.

References:

- Daniel, T. L. (1984). Unsteady aspects of aquatic locomotion. *American Zoologist*, 24, 121 - 134.
- Maresca, C., Favier, D., & Rebont, J. (1979). Experiments on an aerofoil at high angle of incidence in longitudinal oscillations. *Journal of Fluid Mechanics*, 92, 671-690.
- Morison, J. R., O'Brien, M. P., Johnson, J. W., & Schaaf, S. A. (1950). The force exerted by surface waves on piles. *Journal of Petroleum Technology*, 189, 149-154.
- Pai, Y.-C., & Hay, J. G. (1988). A hydrodynamic study of the oscillation motion in swimming. *International Journal of Sport Biomechanics*, 4, 21-37.
- Sarpkaya, T., & Isaacson, M. (1981). *Mechanics of wave forces on offshore structures*. New York: Van Nostrand Reinhold Company.
- Schleihauf, R. E. (1979). A hydrodynamic analysis of swimming propulsion. In J. Terauds, and Bedingfield, E. W. (Ed.), *SWIMMING III* (pp. 70-109). Baltimore, MD: University Park Press.